Dynamics of a $\pm 1/2$ defect pair in a confined geometry: A thin hybrid aligned nematic cell*

Lu Li-Xia(路丽霞)[a)b)c)] and Zhang Zhi-Dong(张志东)[c)†]

[a)] Changchun Institute of Optics, Fine Mechanics and Physics, Chinese Academy of Sciences, Changchun 130033, China
[b)] University of Chinese Academy of Sciences, Beijing 100049, China
[c)] School of Science, Hebei University of Technology, Tianjin 300401, China

(Received 25 June 2014; revised manuscript received 11 September 2014; published online 10 December 2014)

Confined geometry can change the defect structure and its properties. In this paper, we investigate numerically the dynamics of a dipole of $\pm 1/2$ parallel wedge disclination lines in a confined geometry: a thin hybrid aligned nematic (HAN) cell, based on the Landau–de Gennes theory. When the cell gap d is larger than a critical value of 12ξ (where ξ is the characteristic length for order-parameter change), the pair annihilates. A pure HAN configuration without defect is formed in an equilibrium state. In the confined geometry of $d \leq 12\xi$, the diffusion process is discovered for the first time and an eigenvalue exchange configuration is formed in an equilibrium state. The eigenvalue exchange configuration is induced by different essential reasons. When $10\xi < d \leq 12\xi$, the two defects coalesce and annihilate. The biaxial wall is created by the inhomogeneous distortion of the director, which results in the eigenvalue exchange configuration. When $d \leq 10\xi$, the defects do not collide and the eigenvalue exchange configuration originates from the biaxial seeds concentrated at the defects.

Keywords: $\pm 1/2$ defect pair, dynamics, eigenvalue exchange configuration, confined geometry

PACS: 61.30.Jf, 64.70.qj, 61.20.Ja, 61.30.Hn **DOI:** 10.1088/1674-1056/24/2/026102

1. Introduction

Defects are ubiquitous in nature and are important in particle physics, cosmology, and condensed matter physics.[1] This is explained by the importance of the role of defects in the course of different processes (phase transitions, plastic deformations, electronic processes, etc.).[2] Defects in liquid crystals (LCs) affect the manifestations of a number of optical, field, hydrodynamic, and other effects.[2] They have brought some important problems in optoelectric applications[3,4] as well as in fundamental physics. They can trap nanoparticles,[5,6] mediate characteristic interaction between colloidal particles,[6–9] and provide ordered templates for colloidal microassembly.[10–15] Therefore, the location control of topological defects is important for defect-mediated colloidal assembly and guiding polymerization and crystallization in the self-organized nematic order.[6] In recent years, much effort has been devoted to the study of controlling the defect structures in LCs with small scales.[5,6,16–19]

Defects in LCs are topological defects,[2,4] also called disclinations,[20] and induced by singularities in the molecular alignment. The disclinations have the property that they cannot be eliminated by continuous deformation energy. The disclinations in nematic liquid-crystals (NLCs) exhibit in general both point defects with disclination strength $m = \pm 1$ and line defects with $m = \pm 1/2$.[2] They can be divided into two types: wedge disclination (the rotation axis parallel to the disclination line) and twist disclination (the rotation axis normal to the disclination line).[2]

The disclinations appear spontaneously at the isotropic-nematic transition when the $O(3)$ symmetry of the isotropic phase is broken to the $D_{\infty h}$ symmetry of the nematic phase.[21,22] They move in the equilibrating process. Therefore, the dynamics of topological defects in the ordering process has aroused the interest of many researchers and has been largely studied theoretically, numerically, and experimentally over the last few decades.[21–39] All of these studies focused on the relationship between $r(t)$ and t in an annihilation process, where $r(t)$ is the relative distance between two defects in the defect pair and t is the time for the annihilation. Most previous studies have concentrated on investigation of the annihilation of an isolated defect pair.[23–39] However, in a real system, disclinations are never isolated, but subjected to the anchoring forces coming from the substrates of the cell containing the liquid crystal. As a consequence, in a confined geometry, the substrate anchoring is expected to strongly influence the interactions between defect lines. A similar anchoring effect has been invoked to explain the annihilation dynamics of nematic point defects confined in capillary tubes[40] and in hybrid cells.[21,22] However, the behavior of defect lines in a confined geometry remains entirely unexplored.

In this paper, based on our previous study,[18] the relaxation dynamics of a dipole of $m = \pm 1/2$ disclination lines in a

*Project supported by the National Natural Science Foundation of China (Grant No. 11374087) and the Key Subject Construction Project of Hebei Province University.

†Corresponding author. E-mail: zhidong_zhang1961@163.com

© 2015 Chinese Physical Society and IOP Publishing Ltd

thin HAN cell is investigated. The diffusion process is discovered for the first time.

2. Theoretical basis

2.1. Basic equations

Our theoretical argument is based on the Landau–de Gennes theory, in which the orientational order is described by a second-rank traceless and symmetric tensor:[41]

$$\boldsymbol{Q} = \sum_{i=1}^{3} \lambda_i e_i \otimes e_i, \tag{1}$$

where e_i and λ_i are the eigenvectors and the corresponding eigenvalues of $\boldsymbol{Q}$. In the isotropic phase, $\boldsymbol{Q}$ vanishes. When two eigenvalues of $\boldsymbol{Q}$ coincide, the liquid crystal is in a uniaxial state, and $\boldsymbol{Q}$ can be recast in the form of

$$Q_{ij} = S(3n_i \otimes n_j - \delta_{ij}), \tag{2}$$

where S is the uniaxial scalar order parameter, and the unit vector $\boldsymbol{n}$ is the nematic director. When all eigenvalues of $\boldsymbol{Q}$ are different, the liquid crystal is in a biaxial state. The degree of biaxiality of $\boldsymbol{Q}$ can be defined as[41–43]

$$\beta^2 = 1 - \frac{6\left[\mathrm{tr}\left(\boldsymbol{Q}^3\right)\right]^2}{\left[\mathrm{tr}\left(\boldsymbol{Q}^2\right)\right]^3}, \tag{3}$$

β^2 is a convenient parameter for illustrating spatial inhomogeneities of $\boldsymbol{Q}$ and ranges in the interval $[0,1]$. In all uniaxial states, $\beta^2 = 0$, while states with maximal biaxiality correspond to $\beta^2 = 1$.

In the reduced space defined by Schopohl and Sluckin,[44] the dynamics of $\boldsymbol{Q}$ can be described as

$$\frac{\partial \tilde{Q}_{ij}}{\partial \tilde{t}} = \frac{\partial \tilde{f}}{\partial \tilde{Q}_{ij}} - \frac{\partial}{\partial \tilde{x}_k}\frac{\partial \tilde{f}}{\partial \tilde{Q}_{ij,k}}, \tag{4}$$

where $\tilde{f}$ is the free-energy density in the reduced space, $\tilde{t}$ is given by $\tilde{t} = t/\tau$, with $\tau = -\gamma/(BS_c)$. Here, γ is a nematic rotational viscosity. For more details, please refer to our previous study[18] or see Appendix A.

2.2. Geometry of the problem

Consider a pair of defects of disclination strength $m = \pm 1/2$ positioned at $(\pm r_0/2, 0, 0)$, respectively, in a HAN cell with strong anchoring boundary conditions. The substrates are placed at $z = \pm d/2$ of a Cartesian coordinate system. The lengths, d_x and d_y, of the cell along the x axis and the y axis are much larger than d. The nematic director is parallel to the lower substrate and perpendicular to the upper one. The disclination lines are parallel to the y axis as shown in Fig. 1.

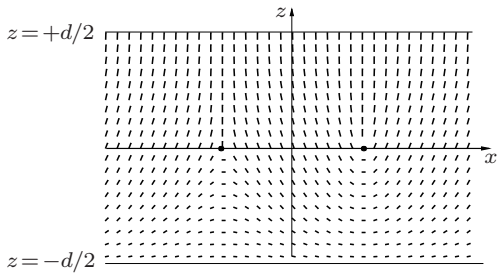


Fig. 1. Geometry of the problem.

2.3. Numerical methods

Time evolution of $\boldsymbol{Q}$ in Eq. (4) is computed in the reduced space by using the two-dimensional finite-difference-iterative-method employed in our previous studies.[18,19] The local values of the scalar order parameter, S, and the director, $\boldsymbol{n}$, can be obtained from $\boldsymbol{Q}(t)$ through its largest eigenvalue and its associated eigenvector, respectively.

The reduced space is discretized into grids with the same interval of $\Delta\tilde{x} = \Delta\tilde{z} = 0.25$. The discretization of time steps given by $5.0\times10^{-3}\tau$ is sufficient to guarantee the stability of the numerical procedure. According to the parameters of 5CB (where CB denotes cyano biphenyl) given in Ref. [45], we have $A_0 = 0.043 \times 10^{-6}$ J/m^3, $B = -1.06 \times 10^{-6}$ J/m^3, $C = 0.87 \times 10^{-6}$ J/m^3, $L_1 = 2.25 \times 10^{-12}$ J/m, $\gamma = 0.077$ Pa·s, and $L_2 + L_3 = 3L_1$.[44] Then $\xi \approx 3.96$ nm and $\tau = 0.54$ μs. The bulk nematic–isotropic transition T_{NI} occurs at $\tilde{A}_C = 1/3$. The scaled temperature is set at $\tilde{A} = 0.25$, which guarantees the system being in the nematic state.

The system is relaxed from the initial condition: two isolated disclinations with $m = \pm 1/2$ situated at a distance of $r_0 = 15\xi$ apart. The initial configuration is

$$\tilde{Q} = T_r \begin{pmatrix} 3\cos^2\theta - 1 & 3\cos\theta\sin\theta & 0 \\ 3\cos\theta\sin\theta & 3\sin^2\theta - 1 & 0 \\ 0 & 0 & -1 \end{pmatrix},$$

where

$$T_r = \frac{S}{S_c} = \frac{3}{4}\left(1 + \sqrt{1 - \frac{8\tilde{A}}{3}}\right).$$

When $x \geq 0$, $\theta = \pi/2 + \phi(\boldsymbol{u})/2$,[46] where $\boldsymbol{u}$ is the distance between the +1/2 singularity and the observation point, $\phi(\boldsymbol{u})$ is the angle between $\boldsymbol{u}$ and the z axis. When $x < 0$, $\theta = \pi/2 - \phi'(\boldsymbol{u}')/2$, where $\boldsymbol{u}'$ is the distance between the $-1/2$ singularity and the observation point, $\phi'(\boldsymbol{u}')$ is the angle between $\boldsymbol{u}'$ and the z axis. θ is the angle between $\boldsymbol{n}$ and the x axis. The strong anchoring conditions on the bounding plates and the free boundaries in the x direction are used, respectively.

3. Results and discussion

When the cell gap d is larger than a critical value of 12ξ, being irrelevant to the initial distance r_0, the pair coalesces and annihilates. A pure HAN configuration without defect is formed in an equilibrium state. When $d \leq 12\xi$, the anchoring forces can squash the biaxial layers into the biaxial wall. Therefore, an eigenvalue exchange configuration is formed when the system is in equilibrium as shown in Fig. 2.

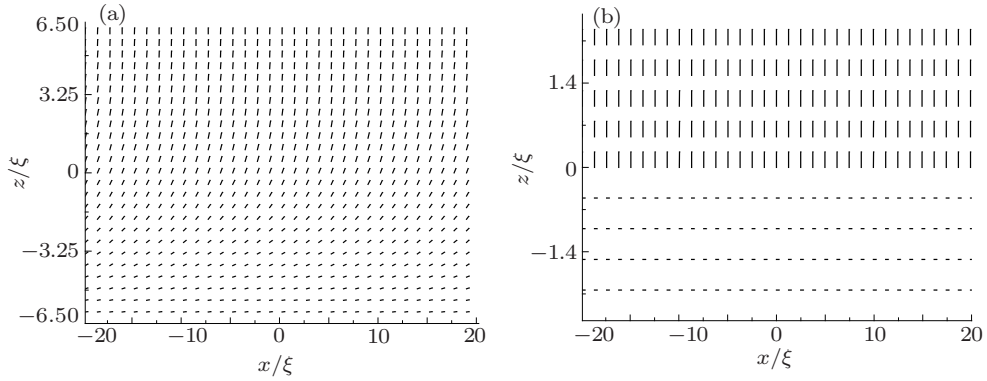


Fig. 2. Director field profile in an equilibrium state of a thin HAN cell with different cell gaps: (a) $d = 13\xi$ (pure HAN configuration) and (b) $d = 5\xi$ (eigenvalue exchange configuration).

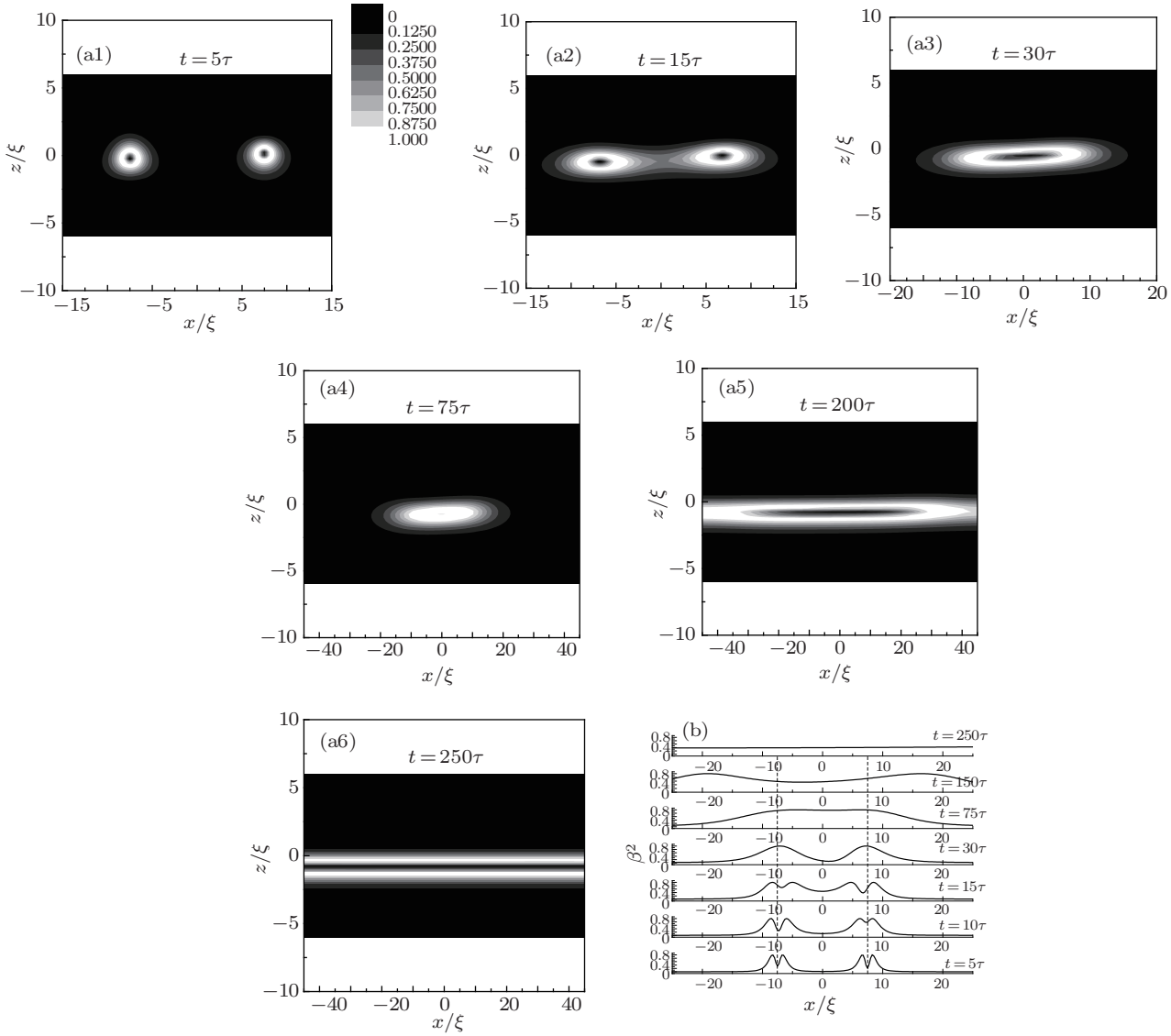


Fig. 3. Values of biaxiality β^2 at different times in a thin HAN cell with $d = 12\xi$: (a) biaxiality β^2 inside the entire cell (different colors represent different values of β^2: white color represents $\beta^2 = 1$, black color denotes $\beta^2 = 0$); (b) biaxiality β^2 across the defect center along the x axis.

The pair annihilation dynamics has been investigated.[21–39] This paper focuses on the dynamic behavior of the pair in a diffusion process.

The pair in a thin HAN cell with different cell gaps exhibits profoundly different behaviors in the diffusion process. In order to give a visual representation of the equilibrium process in a cell with $d = 12\xi$ and investigate the process thoroughly, the time evolutions of the biaxiality, β^2, inside the en-

tire cell and across a defect center along the x axis are plotted in Fig. 3. The z resolution values of the two defect cores are different because of the effects of the anchoring forces and the attraction force. It is random no matter whether the z resolution value of the left defect core is bigger or smaller.

The equilibrium process is divided into two stages. In the first stage, the two defects move toward each other because of the attraction force between them and collide at $t = 30\tau$. Since the two defects are oppositely charged and the total charge is conserved, the defects disappear when they collide. However, the director in the region where the defects collide distorts inhomogeneously. This results in the creation of the biaxial layers when $t \geq 30\tau$ as shown in Fig. 3(a). In this stage, the defects hardly move in the first 10τ then move rapidly until they collide with each other. This is because the attraction force increases with the decrease of the distance between the defects. The biaxial layers induced by the defects diffuse slightly along the x axis. In the second stage, the inhomogeneous distortion region explodes obviously along the x axis. Therefore, the biaxial layers induced by the inhomogeneous distortion of the director explode obviously along the x axis. A biaxial wall is created and an eigenvalue exchange configuration is formed when the system is in equilibrium at $t = 250\tau$. This eigenvalue exchange configuration originates from the biaxial layers induced by the inhomogeneous distortion of the director.

The role of the anchoring forces is strong with the decrease of d, which results in the different behaviors of the pair. When d decreases to 10ξ, the two defects move toward each other, but just cannot collide. At the same time the biaxial layers induced by the defects diffuse very rapidly. They diffuse into the entire cell at $t = 20\tau$. The system transits to an eigenvalue exchange state at $t = 45\tau$ as shown in Fig. 4. The eigenvalue exchange configuration originates from the biaxial seeds concentrated at the defects. The response time decreases to about 24 μs.

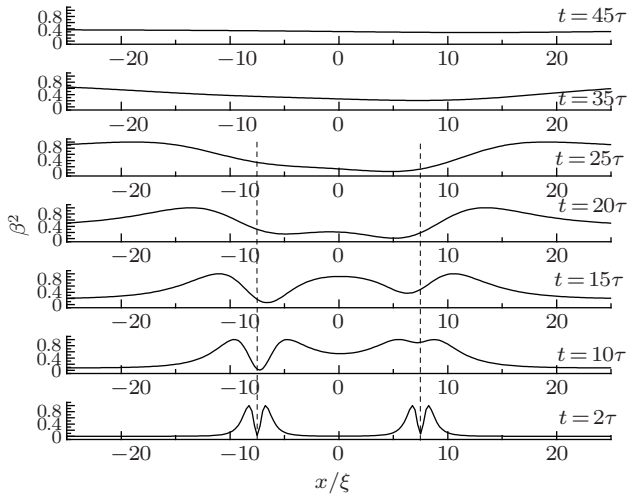


Fig. 4. Time dependences of biaxiality β^2 across the defect center along the x axis with $d = 10\xi$.

The anchoring forces are dominant in the equilibrium process when d is reduced to 5ξ. Therefore, the defects do not move, but diffuse directly into the entire cell rapidly. The system transits to an eigenvalue exchange configuration state when being in equilibrium at $t = 8\tau$ as shown in Fig. 5. The response time is reduced to about 4 μs.

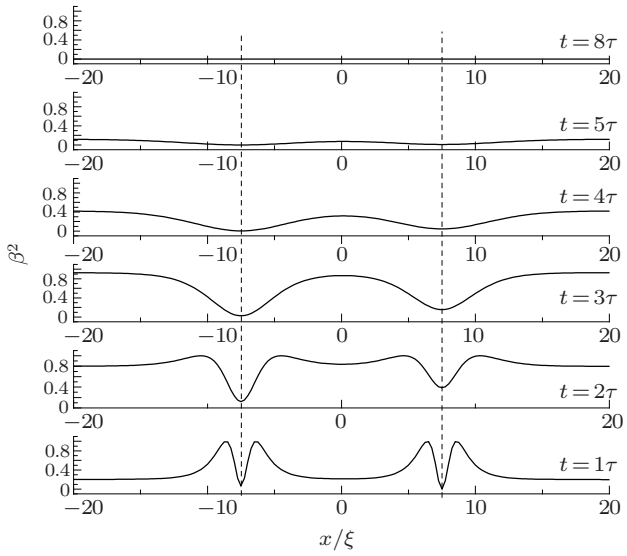


Fig. 5. Time dependences of biaxiality β^2 across the defect center along the x axis with $d = 5\xi$.

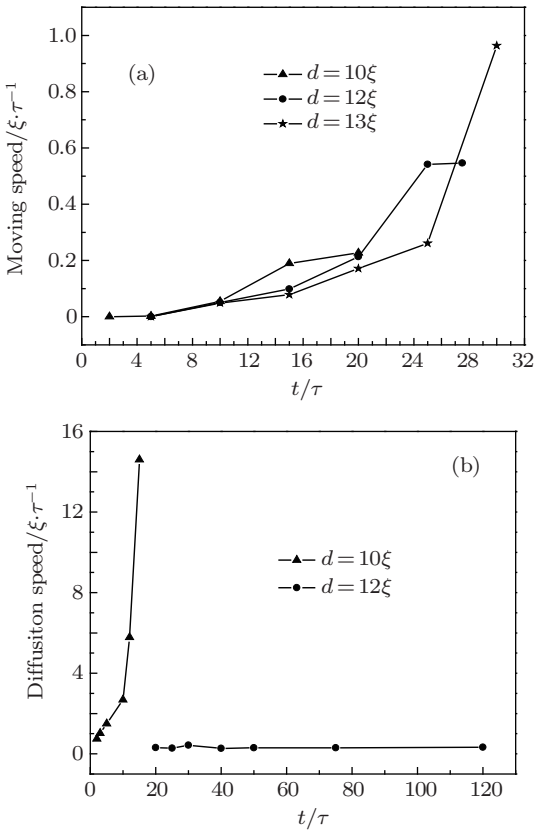


Fig. 6. Variations of (a) defect moving speed and (b) biaxial layers diffusion speed with time t/τ in a HAN cell.

In order to further analyze the different behaviors mentioned above, the defect moving speed and the biaxial layers

diffusion speed each as a function of time for different cell gaps are shown in Figs. 6(a) and 6(b), respectively. The moving speed increases with time in general because of the attraction force between the two defects, $F \propto 1/r(t)$.[46] It is very small (close to zero) and almost irrelevant to d in the first 10τ then increases slightly with the decrease of d. While the diffusion speed increases sharply with the decrease of d. The thinner the cell gap, the stronger the influence of the anchoring forces is. It is the anchoring forces that squash the biaxial layers into the biaxial wall. Therefore, the stronger the influence of the anchoring forces, the bigger the diffusion speed is. This is the reason why the above-mentioned behavior of the pair changes with the decrease of the cell gap.

4. Conclusions

Within Landau–de Gennes theory, we investigate numerically the dynamics of a dipole of $\pm 1/2$ parallel wedge disclination lines in a confined geometry by varying the cell gap d and using the two-dimensional finite-difference-iterative-method. The behavior of the dipole depends on the competition between two kinds of forces: the attraction force between the $\pm 1/2$ parallel disclinations and the anchoring forces coming from the substrates in the confined geometry. The critical gap of $d_c = 12\xi$ is irrelevant to the initial distance r_0. When $d > d_c$, the pair annihilates and a pure HAN configuration without defect is formed. When $d \leq d_c$, an eigenvalue exchange configuration is formed. The eigenvalue exchange configuration is induced by different essential reasons. When $10\xi < d \leq 12\xi$, the biaxial wall is created by inhomogeneous distortion of the director, which results in the eigenvalue exchange configuration. When $d \leq 10\xi$, the eigenvalue exchange configuration originates from the biaxial seeds concentrated at the defects.

The study plays a major role in forming and controlling the topological defects, and has significant academic value for mediation of defects on colloidal particles in NLCs.

Appendix A

The free-energy density f of an NLC without external field can be expressed as

$$f = f_e + f_b, \tag{A1}$$

where f_e and f_b are, respectively, the elastic and the bulk free-energy densities. The former is induced by the inhomogeneous order in LCs. It can be given in the form of

$$f_e = L_1 \frac{\partial Q_{ij}}{\partial x_k}\frac{\partial Q_{ij}}{\partial x_k} + L_2 \frac{\partial Q_{ij}}{\partial x_j}\frac{\partial Q_{ik}}{\partial x_k} + L_3 \frac{\partial Q_{ij}}{\partial x_k}\frac{\partial Q_{ik}}{\partial x_j}, \tag{A2}$$

where L_1, L_2, and L_3 are elastic constants. The latter is a potential that depends on $\boldsymbol{Q}$. It is conventionally described by an expansion in $\boldsymbol{Q}$ up to the fourth order:

$$f_b = A\,\mathrm{tr}\boldsymbol{Q}^2 + \frac{2}{3}B\,\mathrm{tr}\boldsymbol{Q}^3 + \frac{1}{2}C\left(\mathrm{tr}\boldsymbol{Q}^2\right)^2. \tag{A3}$$

Usually it is assumed that $A = A_0(T - T^*)$, where T is the temperature, and T^* is the supercooling temperature. A_0, B, and C are coefficients. The traceless and symmetry of $\boldsymbol{Q}$ are taken into account by introducing the Lagrange parameter tensor:[45] $\Lambda_{ij} = \lambda_0\delta_{ij} - \varepsilon_{ijk}\lambda_k$. The full free-energy functional is

$$f(\boldsymbol{Q}, \boldsymbol{\Lambda}) = f_e + 2\,\mathrm{tr}(\boldsymbol{\Lambda Q}) + f_b. \tag{A4}$$

The calculation can be simplified by dimensionless variables. Here, we follow the rescaling of Schopohl and Sluckin[45] by defining the following dimensionless quantities:

$$\tilde{f} = \frac{f}{B^4/(9C)^3}, \quad \tilde{Q}_{ij} = \frac{Q_{ij}}{S_c}, \quad \tilde{x} = \frac{x}{\xi}, \quad \tilde{y} = \frac{y}{\xi},$$

where $S_c = -B/9C$ is the order parameter at the isotropic-nematic phase transition point and

$$\xi = \sqrt{-\frac{L_1}{BS_C}} = \sqrt{\frac{9CL_1}{B^2}}$$

is the characteristic length for order-parameter change. The dynamics of $\boldsymbol{Q}$ can be described as

$$\frac{\partial \tilde{Q}_{ij}}{\partial \tilde{t}} = \frac{\partial \tilde{f}}{\partial \tilde{Q}_{ij}} - \frac{\partial}{\partial \tilde{x}_k}\frac{\partial \tilde{f}}{\partial \tilde{Q}_{ij,k}}. \tag{A5}$$

i.e., Eq. (4).

References

[1] CarboneG, Lombardo G, Barberi R, Musevic I and Tkalec U 2009 *Phys. Rev. Lett.* **103** 167801
[2] Kurik M V and Lavrentovich O D 1988 *Sov. Phy. Usp.* **31** 196
[3] Tiribocchi A, Gonnella G, Marenduzzo D and Orlandini E 2010 *Appl. Phys. Lett.* **97** 143505
[4] Mermin N D 1979 *Rev. Mod. Phys.* **51** 591
[5] Takuya O and Junichi F 2012 *Nat. Commun.* **3** 701
[6] Ohzono T, Fukuda J I, Suzuki K and Yamaguchi T 2012 *Phys. Rev. E* **86** 030701
[7] Nelson D R 2002 *Nano Lett.* **2** 1125
[8] Tkalec U, Ravnik M, Čopar S, Žumer S and Muševič I 2011 *Science* **333** 62
[9] Ravnik M, Alexander G P, Yeomans J M and Žumer S 2011 *Natl. Acad. Sci. USA* **108** 5188
[10] Voloschenko D, Pishnyak O P, Shiyanovskii S V and Lavrentovich O D 2002 *Phys. Rev. E* **65** 060701(R)
[11] Pires D, Fleury J B and Galerne Y 2007 *Phys. Rev. Lett.* **98** 247801
[12] Fleury J B, Pires D and Galerne Y 2009 *Phys. Rev. Lett.* **103** 267801
[13] Yoon D K, Choi M C, Kim Y H, Kim M W, Lavrentovich O D and Jung H T 2007 *Nat. Mater.* **6** 866
[14] Milette J, Cowling S J, Toader V, Lavigne C, Saez I M, Lennox R B, Goodby J W and Reven L 2012 *Soft Matter* **8** 173
[15] Coursault D, Grand J, Zappone B, Ayeb H, Lévi G, Félidj N and Lacaze E 2012 *Adv. Mater.* **24** 1461
[16] Bisi F, Virga E G and Durand G E 2004 *Phys. Rev. E* **70** 042701
[17] Ambrožič M, Kralj S and Virga E G 2007 *Phys. Rev. E* **75** 031708
[18] Lu L X, Zhang Z D and Zhou X 2013 *Acta Phys. Sin.* **62** 226101 (in Chinese)
[19] Zhou X and Zhang Z D 2013 *Int. J. Mol. Sci.* **14** 24135
[20] Gennes P G and Prost J 2008 *The Physics of Liquid Crystals*, 2nd edn. (Beijing: Science Press) p. 166

[21] Minoura K, Kimura Y, Ito K, Hayakawa R and Miura T 1998 *Phys. Rev. E* **58** 643
[22] Bogi A, Martinot-Lagarde P, Dozov I and Nobili M 2002 *Phys. Rev. Lett.* **89** 225501
[23] Shiwaku T, Nakai A, Hasegawa H and Hashimoto T 1990 *Macromolecules* **23** 1590
[24] Chuang I, Turok N and Yurke B 1991 *Phys. Rev. Lett.* **66** 2472
[25] Pargellis A, Turok N and Yurke B 1991 *Phys. Rev. Lett.* **67** 1570
[26] Pargellis A N, Finn P, Goodby J W, Panizza P, Yurke B and Cladis P E 1992 *Phys. Rev. A* **46** 7765
[27] Chuang I, Yurke B, Pargellis A N and Turok N 1993 *Phys. Rev. E* **47** 3343
[28] Ding D K and Thomas E L 1994 *Mol. Cryst. Liq. Cryst.* **241** 103
[29] Pargellis A N, Mendez J, Srinivasarao M and Yurke B 1996 *Phys. Rev. E* **53** R25
[30] Minoura K, Kimura Y, Ito K and Hayakawa R 1997 *Mol. Cryst. Liq. Cryst.* **302** 345
[31] Wang W, Shiwaku T and Hashimoto T 1998 *J. Chem. Phys.* **108** 1618
[32] Svensek D and Žumer S 2002 *Phys. Rev. E* **66** 021712
[33] Tóth G, Denniston C and Yeomans J M 2002 *Phys. Rev. Lett.* **88** 105504
[34] Bradač Z, Kralj S, Svetec M and Žumer S 2003 *Phys. Rev. E* **67** 050702(R)
[35] Dierking I, Marshall O, Wright J and Bulleid N 2005 *Phys. Rev. E* **71** 061709
[36] Svetec M, Kralj S, Bradac Z and Žumer S 2006 *Eur. Phys. J. E* **20** 71
[37] Guimarães R R, Mendes R S, Fernandes P R G and Mukai H 2013 *J. Phys.: Condens. Matter* **25** 404203
[38] Giomi L, Bowick M J, Ma X and Marchetti M C 2013 *Phys. Rev. Lett.* **110** 228101
[39] Ribeiro H V, Guimarães R R, Teixeira-Souza R T, Mukai H, Fernandes P R G, Lenzi E K and Mendes R S 2013 *Phys. Rev. E* **87** 054501
[40] Bajc J, Peroli G G , Virga E G and Žumer S 2002 *Liquid Cryst.* **29** 213
[41] Bisi F, Gartland E C, Rosso R and Virga E G 2003 *Phys. Rev. E* **68** 021707
[42] Barberi R, Ciuchi F, Durand G, Iovane M, Sikharulidze D, Sonnet A and Virga E 2004 *Eur. Phys. J. E* **13** 61
[43] Lombardo G, Ayeb H and Barberi R 2008 *Phys. Rev. E* **77** 051708
[44] Schopohl N and Sluckin T J 1987 *Phys. Rev. Lett.* **59** 2582
[45] Qian T Z and Sheng P 1997 *Phys. Rev. E* **55** 7111
[46] Gennes P G and Prost J 2008 *The Physics of Liquid Crystals*, 2nd edn. (Beijing: Science Press) p. 165